Phase Envelope Calculations for Hydrocarbon-Water Mixtures

Niels Lindeloff, SPE, Calsep, and **Michael L. Michelsen,** IVC-SEP, Technical U. of Denmark

Summary

The present work describes how the pressure-temperature phase diagrams for hydrocarbon-water mixtures can be calculated. This requires a thermodynamic model that can account for the polar interactions caused by the aqueous compounds and an algorithm that can trace the two- and three-phase boundaries encountered in such systems. Models and algorithms that can handle this task are described. The paper further describes a number of examples in which the methods are applied.

Introduction

Development of high-pressure high-temperature (HP/HT) fields and the increased use of subsea completions and tiebacks of satellite fields result in transport of unprocessed well streams, where mixtures of hydrocarbons, water, and hydrate inhibitors are transported in pipelines at high pressures. In HP/HT gas condensate fields, large amounts of water can be dissolved in the hydrocarbon phases, but may separate out in the well stream during production. Because of cooling in the subsea environment, hydrate formation is a concern, and fluid inhibitors such as methanol are often added to the well stream. The mutual solubility of hydrocarbons, water, and other polars is considerable in such systems. Furthermore, both oil and condensate systems may exhibit behavior in which three phases are present at low temperatures.

Being able to properly simulate this type of systems puts some additional requirements on the simulation model, both in terms of thermodynamic model and calculation algorithms. Operating conditions to be accounted for range from bottomhole pressures and temperatures, which can be on the order of 200°C/400°F and 1000 bar/15,000 psi and down to deepwater seabed temperatures on the order of 0°C/ 32°F and low pressure. The two-parameter Equations of State (EOS), such as the Soave-Redlich-Kwong (SRK)[1] and the Peng-Robinson (PR)[2] models, have gained widespread acceptance in the petroleum industry for their ability to correlate hydrocarbon system behavior up to high pressures. The limitations of the classical formulation of the cubic EOS are well understood, and include failure to correctly handle polar systems in which local composition effects dominate, and problems in correlating system behavior over a large temperature range. These problems have been addressed previously in literature. A brief review will be given of the approaches taken here to remedy the mentioned shortcomings. In terms of algorithms, two fundamental types are required. These are a multiphase flash and a phase envelope algorithm, which can trace boundaries between the different regions of the phase diagram. Multiphase flash algorithms have been described elsewhere[3]; also, the construction of an envelope for two-phase hydrocarbon systems is known technology, and an account for how this is done can be found in literature.[4] The problem is greatly complicated by the introduction of an aqueous phase or a third hydrocarbon phase, and the concepts applied to handle this complexity are the topic of the present paper.

Thermodynamic Modeling Approach

A phase envelope covering hydrocarbon as well as aqueous phase boundaries can be constructed only if all phases are described using the same thermodynamic model. Hydrocarbon phases are most conveniently described using a classical cubic EOS. A classical EOS is, however, not able to represent mixtures of hydrocarbons and polar components. This is a requirement in the present context. Finally, the model should be able to satisfactorily correlate the mutual solubilities of hydrocarbon and water phases. This leads to four model requirements that have to be met:

1. Ability to represent mixtures containing polar components.
2. Flexibility to allow correlation of solubility data.
3. Same model applicable to all phases present.
4. Model can reduce to classical cubic EOS in the absence of polar compounds.

Models like the Wong-Sandler model,[5] the MHV-1, and the MHV-2[6] fulfill all criteria except Requirement 4. Failure to comply with the last requirement means that model-specific binary interaction parameters will have to be estimated for each hydrocarbon-hydrocarbon binary pair. In view of the complexity of the C_{7+}-fraction of petroleum fluids, this was considered undesirable, because a new C_{7+} characterization procedure would have to be developed for that purpose. Søreide and Whitson[7] have thus proposed to use the EOS for all phases present, but to apply different interaction coefficients for the hydrocarbon phases and for the aqueous phase. This model approach meets Requirement 4 but not 3, which means that an objective criterion for identifying an aqueous phase is required. This is not possible at all conditions encountered when tracing phase boundaries, in particular near critical points. The Cubic-Plus-Association EOS[8] and the original Huron and Vidal model[9] are approaches that reduce to the classical EOS for a proper selection of interaction parameters and thus fulfill all four criteria.

The present work will use the original Huron and Vidal model to exemplify the application of the presented algorithm. The ability of the Huron and Vidal model to correlate the mutual solubility of hydrocarbon and aqueous phases in a reasonable way has been verified by Pedersen *et al.*[10,11] and Sørensen *et al.*[12] No attempt has been made to compare model performance with the other approaches discussed.

The classical quadratic mixing rule for the EOS a-parameter is shown in Eq. 1.

$$a=\sum_{i=1}^{N}\sum_{j=1}^{N}z_iz_ja_{ij}, \qquad (1)$$

where a_{ij} is defined in Eq. 2:

$$a_{ij}=(a_ia_j)^{1/2}(1-k_{ij}). \qquad (2)$$

In these equations, a_i and a_j = the pure component a-parameters for the corresponding species, z_i and z_j the corresponding mole fractions, and k_{ij} the binary interaction coefficient. N = the number of components in the mixture. A model fulfilling Requirement 4 must be able to reduce to Eq. 1 for appropriate selection of interaction parameters. As discussed in the following, the Huron and Vidal model has this capacity.

The Huron and Vidal a-parameter mixing rule takes the following form:

$$a=b\left[\sum_{i=1}^{N}\left(z_i\frac{a_i}{b_i}\right)-\frac{G_\infty^E}{\ln 2}\right]. \qquad (3)$$

In this equation, z = the mole fraction, a and b = the equation of state parameters, i = the component index, and G_∞^E = the excess Gibbs energy at infinite pressure. G_∞^E in this case comes from a modified NRTL mixing rule,[7] as shown in Eq. 4.

Copyright © 2003 Society of Petroleum Engineers

This paper (SPE 85971) was revised for publication from paper SPE 77770, prepared for presentation at the 2002 SPE Annual Technical Conference and Exhibition, San Antonio, Texas, 29 September–2 October. Original manuscript received for review 13 January 2003. Revised manuscript received 2 May 2003. Manuscript peer approved 18 May 2003.

$$\frac{G^E_\infty}{RT} = \sum_{i=1}^{N} z_i \frac{\sum_{j=1}^{N} \tau_{ji} b_j z_j \exp(-\alpha_{ji}\tau_{ji})}{\sum_{k=1}^{N} b_k z_k \exp(-\alpha_{ki}\tau_{ki})}. \quad \ldots\ldots\ldots\ldots (4)$$

α_{ij} = nonrandomness parameter to account for the local composition effects (local mole fraction may differ from overall mole fraction), while α_{ij}=0 corresponds to a completely random mixture. The parameter τ_{ij} accounts for the interaction between molecules through the following expression:

$$\tau_{ji} = \frac{g_{ji} - g_{ii}}{RT}, \quad \ldots\ldots\ldots\ldots (5)$$

where g_{ji} = an energy parameter characteristic of the *j-i* interaction. A very useful feature of the Huron-Vidal mixing rule is that it reduces to the classical quadratic mixing rule from Eqs. 1 and 2 when the α and g parameters are selected as follows:

$$\alpha_{ij} = 0, \quad \ldots\ldots\ldots\ldots (6)$$

$$g_{ii} = \frac{a_i}{b_i} \ln 2, \quad \ldots\ldots\ldots\ldots (7)$$

$$g_{ji} = -2\frac{\sqrt{b_i b_j}}{b_i + b_j}\sqrt{g_{ii} g_{jj}}(1 - k_{ij}), \quad \ldots\ldots\ldots\ldots (8)$$

where k_{ij} = the binary interaction parameter from the classical *a*-parameter mixing rule discussed above. The mixing rule of Eq. 3 reduces to Eq. 1, and Requirement 4 is fulfilled. This means that α_{ij}, g_{ij}, and g_{ji} for hydrocarbon-hydrocarbon binaries can be calculated from Eqs. 6 through 8, and model-specific interaction parameters will only have to be estimated for binaries of the types hydrocarbon-polar and polar-polar.

Phase Envelope Algorithm

Pedersen *et al.*[10] have previously presented an algorithm for calculating phase boundaries in three-phase mixtures containing hydrocarbons and aqueous components such as water, alcohols, and glycols. The scope of this algorithm was more limited, because the incipient phase had to be a hydrocarbon phase, and only the temperature range from approximately 250 to approximately 450 K was considered.

The present algorithm, in contrast, is capable of automatic generation of the entire phase diagram (i.e., the lines that separate the regions in the *P,T*-plane where 1, 2, and 3 phases, respectively, are present). A generic PT phase diagram is shown in **Fig. 1.** The key steps in the new algorithm are:

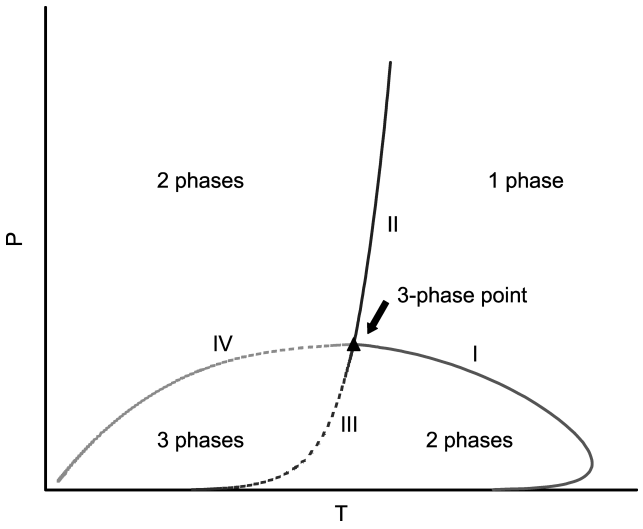

Fig. 1—Generic PT phase diagram for a hydrocarbon-water system.

1. Tracing the dewline segments that separate the single-phase region from the two-phase region (Lines I and II in Fig. 1).

2. Determining the three-phase points on the dewline. These are the points where the overall composition is at equilibrium with two incipient phases.

3. Tracing the phase boundaries that separate the two-phase region from the three-phase region (Lines III and IV in Fig. 1). These phase boundaries emerge from the three-phase points or exist as isolated lines.

Let the overall composition of the *N*-component mixture be **z**. Points on the dewline satisfy the following set of equations:

$$\ln w_i + \ln \varphi_i(\mathbf{w}) - \ln z_i - \ln \varphi_i(z) = 0, \qquad i = 1,2,\ldots,N, \ldots (9)$$

$$\sum_{i=1}^{N} w_i - 1 = 0, \quad \ldots\ldots\ldots\ldots (10)$$

where **w** = the composition of the incipient phase. An additional requirement is that the mixture is stable. Stability is investigated by minimizing the tangent plane distance.[13] The minima are found at compositions **y** where

$$\ln y_i + \ln \varphi_i(\mathbf{y}) - \ln z_i - \ln \varphi_i(\mathbf{z}) = k, \quad i = 1,2,\ldots,N, \ldots\ldots (11)$$

$$\sum_{i=1}^{N} y_i - 1 = 0, \quad \ldots\ldots\ldots\ldots (12)$$

and stability requires that k is nonnegative at all solutions to Eq. 11.

The calculation of the dewline is initiated by calculating the dewpoint at atmospheric pressure. Initial estimates are generated in a similar manner as in Pedersen *et al.*[10] For the vapor phase we take φ_i^v for a hydrocarbon component in a hydrocarbon liquid or for an aqueous component in a water-rich liquid, $\ln\varphi_i^l = \ln\varphi_i^{\text{Wilson}}$ is used, and finally, for aqueous components in a hydrocarbon liquid or hydrocarbon components in an aqueous liquid, use $\ln\varphi_i^l = \ln\varphi_i^{\text{Wilson}} + 10$. Here, the Wilson *K*-factor approximation is utilized:

$$\ln \varphi_i^{\text{Wilson}} = \ln\left(\frac{P_{ci}}{P}\right) + 5.373(1 + \omega_i)\left(1 - \frac{T_{ci}}{T}\right), \quad \ldots\ldots\ldots (13)$$

where T_{ci} = the critical temperature, P_{ci} = the critical pressure, and ω_i = the acentric factor for the *i*th component. This gives two sets of liquid-phase fugacities, $\ln\varphi_i^{l,\text{hc}}(T,P)$ and $\ln\varphi_i^{l,aq}(T,P)$ that apply for a hydrocarbon phase and an aqueous phase, respectively.

Substituting the above expressions in Eq. 9 results in

$$\sum_{i=1}^{N} x_i = \sum_{i=1}^{N} \frac{z_i}{\varphi_i^l(T,P)} = 1, \quad \ldots\ldots\ldots\ldots (14)$$

which can be solved for the temperature. The choice of a hydrocarbon liquid or an aqueous liquid will give different results. The one yielding the higher temperature is chosen. The full set of Eqs. 9 and 10 is subsequently solved by a partial Newton's method, in which the composition dependence of the fugacity coefficients is not taken into account. Finally, the converged solution is tested for stability as follows: A trial phase composition is generated from

$$X_i = z_i \frac{\varphi_i(\mathbf{z})}{\varphi_i^{l*}}, \quad x_i = \frac{X_i}{\sum_j X_j}, \quad \ldots\ldots\ldots\ldots (15)$$

where φ_i^{l*} represents the Wilson-based fugacities for the phase type that was not used in the high-temperature solution of Eq. 14. The stability equations are converged by successive substitution[13] and, if necessary, Newton's method. In case the solution determined initially is unstable, the phase type for the initial liquid is changed, and a revised (higher) dewpoint temperature is calculated.

Subsequent calculation of points on the dewline at higher pressures are performed as described by Michelsen.[4] This results in the construction of Line I in Fig. 1. Each calculated point is checked for stability as described above. If instability is discovered, the next step is to determine the corresponding three-phase point, where the overall composition **z** is at equilibrium with two incipi-

ent phases. The equations that must be satisfied at a three-phase point are

$$\ln w_i + \ln \varphi_i(\mathbf{w}) - \ln z_i - \ln \varphi_i(\mathbf{z}) = 0$$

$$\ln x_i + \ln \varphi_i(\mathbf{x}) - \ln z_i - \ln \varphi_i(\mathbf{z}) = 0$$

$$\sum_{i=1}^{N} x_i - 1 = 0 \quad \ldots\ldots\ldots\ldots\ldots\ldots (16)$$

$$\sum_{i=1}^{N} w_i - 1 = 0$$

Solution of these is first attempted through a partial Newton's method, where, again, the partial composition derivatives of the fugacity coefficients are disregarded. Initial estimates of the phase compositions are available from the dewpoint calculations (**w**) or the stability analysis (**x**). Final convergence is obtained by means of a full Newton's method.

The phase compositions, temperature, and pressure at the 3-phase points are recorded for later use, and the calculation of the dewline is continued after switching the phase types for the incipient phases. Thus, if the initial branch of the dewline had a hydrocarbon liquid as the incipient phase, calculations continue after the three-phase point with an aqueous phase as the incipient. For this branch, the hydrocarbon-phase Wilson expressions are used to initiate the stability analysis. This corresponds to Line II in Fig. 1. In case instability is detected again, the new three-phase point is calculated and the construction continued. The dewline terminates when the pressure exceeds a specified upper limit. Cases in which no three-phase point, a single point, or two points are found, are common.

The next step is to trace the three-phase phase boundaries that initiate from the three-phase points. Each three-phase point "generates" two three-phase lines, one with an incipient hydrocarbon phase (Line IV) and one with an incipient aqueous phase (Line III). It is convenient to use the incipient phase as the reference phase for the equilibrium factors. Let the incipient phase composition be **w** and that of the other phases **x** and **y,** and let β be the fraction of total moles in the **y** phase. Defining equilibrium factors,

$$K_{ix} = \frac{x_i}{w_i}, \qquad K_{iy} = \frac{y_i}{w_i}, \quad \ldots\ldots\ldots\ldots\ldots\ldots (17)$$

the overall material balance,

$$z_i = \beta \quad y_i + (1-\beta)\, x_i \quad \ldots\ldots\ldots\ldots\ldots\ldots (18)$$

allows all phase compositions to be expressed in terms of these variables, as with

$$w_i = \frac{z_i}{\beta K_{iy} + (1-\beta)\, K_{ix}}, \quad x_i = K_{ix} w_i, \quad y_i = K_{iy} w_i. \quad \ldots\ldots\ldots (19)$$

The equations that apply along the phase boundary are

$$\ln K_{iy} + \ln \varphi_i(\mathbf{y}) - \ln \varphi_i(\mathbf{w}) = 0$$

$$\ln K_{ix} + \ln \varphi_i(\mathbf{x}) - \ln \varphi_i(\mathbf{w}) = 0\,, \quad \ldots\ldots\ldots\ldots\ldots\ldots (20)$$

$$\sum_i w_i - 1 = 0\,, \quad \sum_i (y_i - x_i) = 0$$

together with a specification equation that specifies the value of *T, P,* β, or one of the *K*-factors.

As independent variables, we use the logarithm of the *K*-factors, *T* and *P,* and the phase fraction. The sets of equations are solved by Newton's method, and the extrapolation method described by Michelsen[4] for two-phase phase boundaries is used for generating initial estimates.

The initial point on the three-phase line is the three-phase point, corresponding to β=1, **y=z,** and the choice of incipient phase decides which of the branches to follow. The tracing of the three-phase line is terminated if computations return to a three-phase point, or if an upper or a lower prescribed value of the pressure is exceeded.

Finally, in case no three-phase point is found on the dewline, a search for an inner, isolated three-phase region as described earlier by Pedersen *et al.*[10] is carried out.

The procedure of Michelsen,[4] in addition, enables locating critical points on the dewline and on the three-phase phase boundaries. For critical points on a three-phase boundary, the incipient phase will always be one of the critical phases. One may therefore check for passing a critical point by a sign change in the log *K* for either the **x**- or the **y**-phase.

These phases cannot become mutually critical except in the rare coincidence of a critical three-phase point. The stepsize selection procedure of Michelsen is designed to place the specifications at a "safe" distance from the critical point, because the set of equations becomes very ill-conditioned in the critical region. If specifications very close to the critical point are attempted, it may not be possible to converge the set of equations (Eq. 20), because round-off errors corrupt the calculated Jacobian.

One situation that cannot be handled by appropriate step selection is that of a near-critical three-phase point. In rare cases it has been impossible to converge Eq. 16, because one of the phase pairs was almost critical. The solution used to overcome this problem is to perform the calculations in quadruple precision, if this is deemed necessary. Such calculations are extremely costly, the performance penalty being about a factor of 20. Therefore the switch to quadruple precision is only made near a critical point. The criterion for near-criticality is defined as when the *K*-factors for one phase all fall in the range from 0.9 to 1.1.

Examples

The examples presented have been selected with a view to obtaining behavior that tests the algorithm to the limits, but are nonetheless compositions that could be encountered at different stages in a production scenario. The model has been verified against data at relevant operating conditions,[10,11] but it should be noted that no data are available to verify the model at the very high temperatures that are also included in the phase diagrams shown.

The uncharacterized compositions of the fluids considered are given in **Table 1.** In all cases the fluids were characterized following the principles of the Pedersen[14] method, and calculations were carried out using the SRK-Peneloux EOS with the Huron and Vidal mixing rule implemented as described previously in this work.

The first example, Fluid A, concerns a dry gas with a low water content, 500 ppm (wt) of water. The resulting phase diagram has been plotted in **Fig. 2.** In this case the water dewline separates the single-phase vapor region from a two-phase vapor-liquid water region. At lower temperatures, the hydrocarbon dewline separates the two-phase region from a three-phase region in which vapor, liquid hydrocarbon, and liquid water phases coexist. The algorithm in this case starts by tracing the water dewline. Because no three-

TABLE 1—COMPOSITIONS OF THE FOUR FLUIDS

	Fluid A	Fluid B	Fluid C	Fluid D
N_2	0.34	0.00	1.12	0.30
CO_2	0.84	2.79	1.00	3.40
C_1	89.95	71.51	47.00	71.70
C_2	5.17	5.77	4.00	8.00
C_3	2.04	4.10	2.77	3.80
iC_4	0.36	1.32	0.51	0.80
nC_4	0.55	1.60	2.15	1.50
iC_5	0.14	0.82	0.84	0.70
nC_5	0.10	0.64	1.15	0.80
C_6	0.01	1.05	1.84	1.00
C_{7+}	0	10.40	37.58	8.00
M_{7+}	n/a	191	251	156
ρ_{7+}	n/a	0.82	0.88	0.815

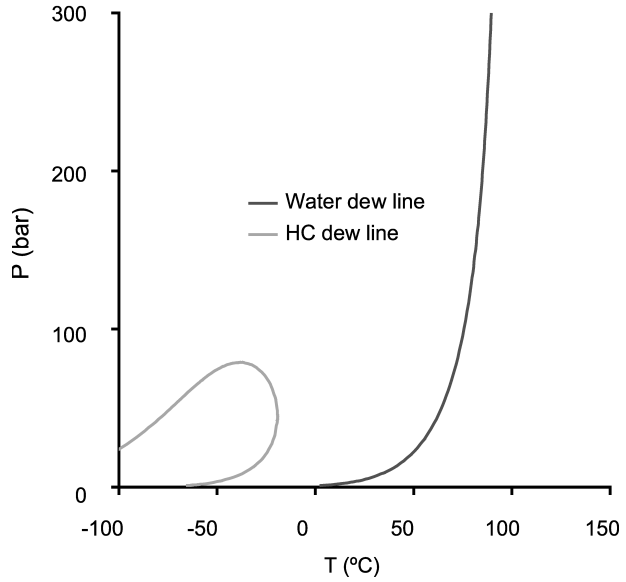

Fig. 2—Phase diagram for Fluid A with 500 ppm water.

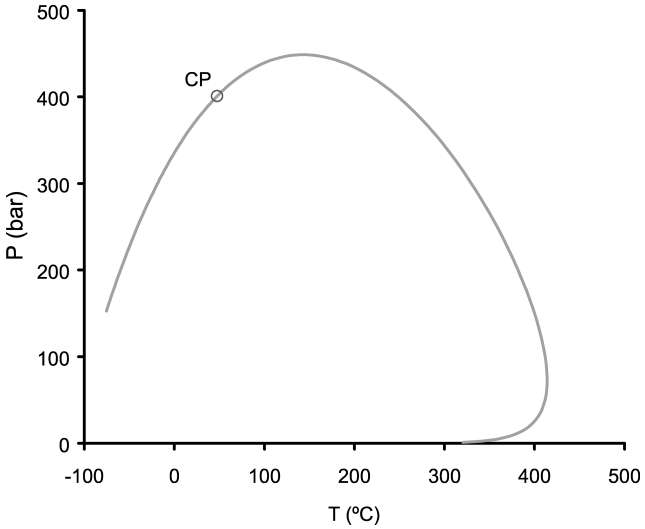

Fig. 3—Phase envelope for water-free condensate, Fluid B.

phase points are encountered on this line, the search for an inner three-phase line is used to locate the hydrocarbon dewline.

The second example, Fluid B, is a gas condensate. The water-free hydrocarbon phase envelope for this fluid is shown in **Fig. 3.** Adding water to the system, corresponding to an 8% watercut at stock-tank conditions, leads to a phase diagram as shown in **Fig. 4.** Lines marked *W* are phase boundaries where the incipient phase is aqueous. Boundaries where the incipient phase is carbon-rich are marked *H*. In Fig. 4, the water dewline crosses the hydrocarbon dewline, and consequently, when tracing the first two-phase dewline, the algorithm locates a three-phase point, marked by a triangle on the figure. The three-phase point in effect defines the starting point for locating the remaining three curves. Compared to the water-free phase envelope, the presence of the water mainly affects the three-phase hydrocarbon dewline. This effect can become very pronounced at higher watercuts, as is illustrated in **Fig. 5.** In Fig. 5, the mutual solubility of water and hydrocarbons leads to a significant deformation of the region where two hydrocarbon phases are present. This effect is most dramatic at extremely high temperatures, but will also affect the curves at temperatures representative of normal operating conditions. The presence of methanol will further have a large effect on the mutual solubilities of hydrocarbons and aqueous compounds. This is illustrated in **Fig. 6,** where the aqueous phase contains 50 wt% methanol, corresponding to a 60% watercut at stock-tank conditions. In this case, the two-phase hydrocarbon dewline denoted 2-*H* separates the single-phase vapor region from a vapor-hydrocarbon liquid region. Moving toward lower temperature at pressures below the critical point, a three-phase water dewline (3-*W*) is encountered, which ends in a critical point. Moving past the critical point, a three-phase hydrocarbon dewline denoted 3-*H* borders the other side of the three-phase region. Above the 3-*H* line, vapor coexists with a liquid water phase. The effect of having an aqueous phase with a significant methanol content present is further illustrated for Fluid C in **Fig. 7.** In this case, the fluid is mixed with water and methanol in a proportion corresponding to a 60% watercut at stock-tank conditions. Approximately 30 wt% methanol was added to the water. In Fig. 7, the phase diagram for this mixture is compared to the phase diagram for the water-free Fluid C, illustrated by the dotted line. The plot clearly demonstrates that a dramatic effect is to be expected both for the hydrocarbon dewline and for the hydrocarbon bubble line in such a system.

A final example will serve to illustrate the situation in which more than one three-phase point is encountered. **Fig. 8** shows the phase diagram for Fluid D mixed with water corresponding to a 75% water cut at stock-tank conditions. Fluid D is a gas condensate. Some of the features discussed for this phase diagram will

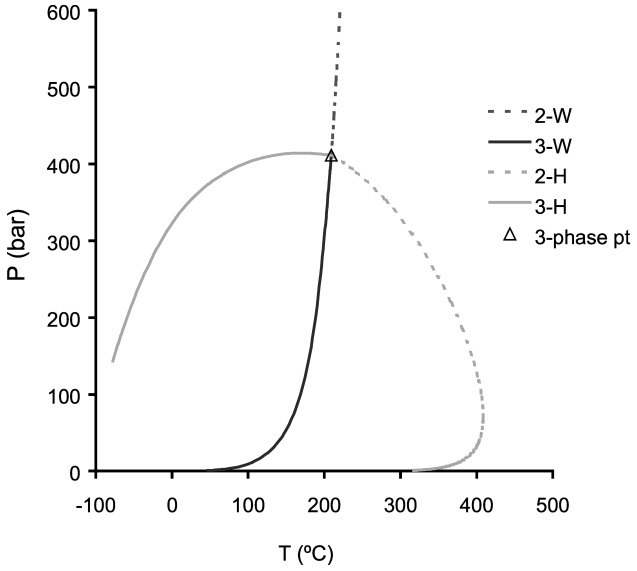

Fig. 4—Phase diagram for Fluid B with 8% water cut.

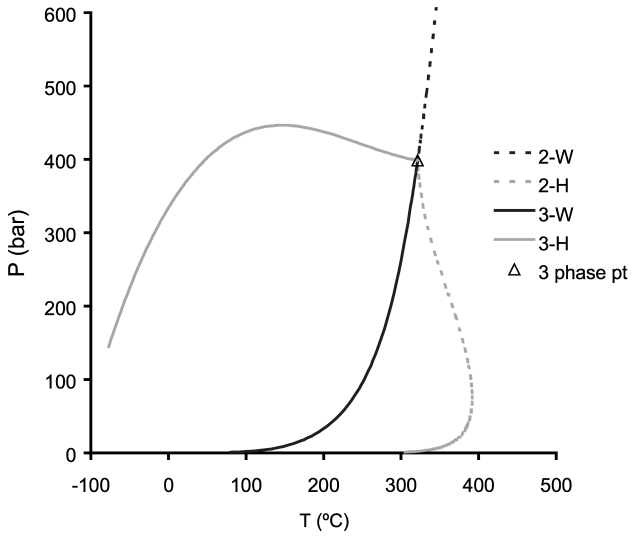

Fig. 5—Fluid B with 40% water cut.

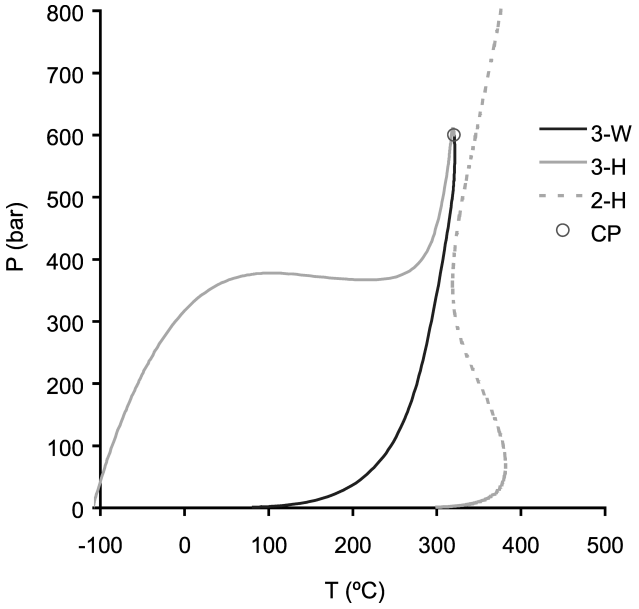

Fig. 6—Fluid B with water and MeOH corresponding to a 60% water cut.

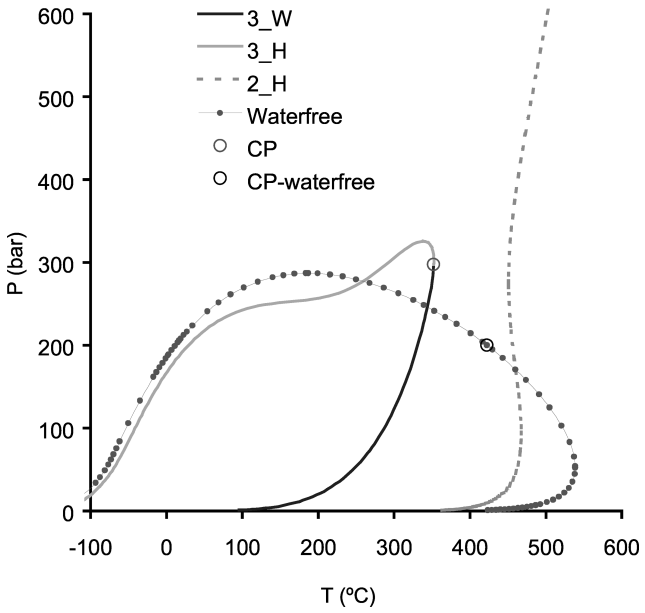

Fig. 7—Comparison of phase diagrams for Fluid C with and without aqueous phase present.

occur outside the temperature range that is relevant for normal operating conditions. They are nonetheless of interest, because the stepwise nature of the algorithm makes it necessary to consider these parts of the phase diagram as well. The algorithm starts by tracing the two-phase dewlines, which in turn leads to the location of the two three-phase points. Subsequently, the three-phase lines are traced. The lines emerging from the three-phase point with the lower pressure has two separate branches, whereas the lines from the high-pressure three-phase point forms a closed curve. An interesting feature for this fluid system is the deformation of the hydrocarbon dewline around the "low-pressure" three-phase point. This is caused by an increase in solubility of the hydrocarbons around the three-phase point, whereas for Fluid B a decrease in solubility was observed. The closed three-phase area at high temperature and pressure is a region where a hydrocarbon liquid is forming, in addition to the vapor and aqueous phases already present.

Conclusions

An algorithm for automatic calculation of phase boundaries in three-phase systems with a hydrocarbon liquid and an aqueous liquid has been developed. In contrast to earlier algorithms, the complete phase diagram, including two-phase and multiphase critical points, is generated without user intervention.

The complex behavior observed for some of these systems emphasizes the need for thermodynamic models that can properly account for the hydrocarbon-water interactions.

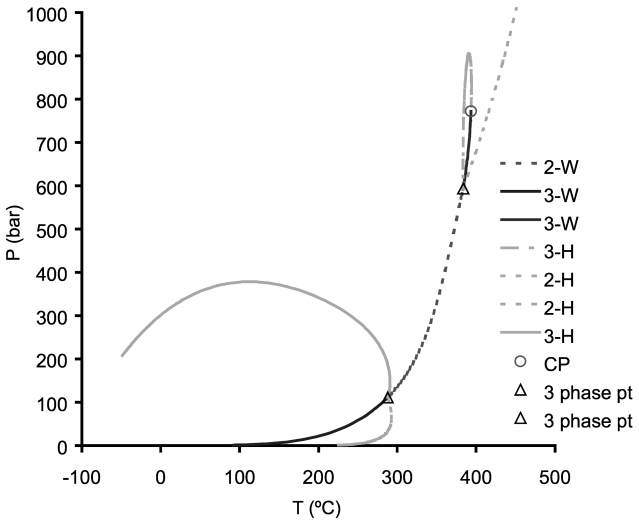

Fig. 8—Phase diagram for Fluid D with a 75% water cut.

Nomenclature

a = attractive parameter of cubic EOS
b = covolume parameter of cubic EOS
g_{ji} = interaction energy between species j and i
G^E = molar excess Gibbs energy
k_{ij} = binary interaction coefficient
K_i = equilibrium factor, Eq. 18
M = molecular weight
N = number of components in mixture
P = pressure
R = gas constant
T = temperature
w_i, x_i, y_i = phase mole fractions of component i
z_i = overall mole fraction of component i
α_{ij} = nonrandomness parameter
β = vapor fraction
ρ = density (g/cm^3)
τ_{ji} = parameter in NRTL equation, Eq. 5
φ_i = fugacity coefficient, component i
ω_i = acentric factor, component i

Symbols in bold denote vectors.

References

1. Soave, G.: "Equilibrium Constants From a Modified Redlich-Kwong Equation of State," *Chem. Eng. Sci.* (1972) **27,** 1197.
2. Peng, Y. and Robinson, D.B.: "A New Two-Constant Equation of State," *Ind. Eng. Chem. Fundam.* (1976) **15,** 59.
3. Michelsen, M.L.: "Calculation of Multiphase Equilibrium," *Comp. Chem. Eng.* (1994) **18,** 545.
4. Michelsen, M.L.: "Calculation of Phase Envelopes and Critical Points for Multicomponent Mixtures," *Fluid Phase Equilibria* (1980) **4,** 1.
5. Wong, D.S.H. and Sandler, S.I.: "A Theoretically Correct Mixing Rule for Cubic Equations of State," *AICHE Journal* (1992) **38,** 671.
6. Michelsen M.L.: "A Modified Huron-Vidal Mixing Rule for Cubic Equations of State," *Fluid Phase Equilibria* (1990) **60,** 213.

7. Søreide, I. and Whitson, C.H.: "Peng-Robinson Predictions for Hydrocarbons, CO_2, N_2, and H_2S with Pure Water and NaCl Brine," *Fluid Phase Equilibria* (1992) **77,** 217.
8. Yakoumis, I.V. *et al.:* "Vapor-liquid equilibria for alcohol/hydrocarbon systems using the CPA Equation of State," *Fluid Phase Equilibria* (1997) **130,** 31.
9. Huron, M.J. and Vidal, J.: "New Mixing Rules in Simple Equations of State for Representing Vapor-Liquid-Equilibria of Strongly Non-Ideal Mixtures," *Fluid Phase Equilibria* (1979) **3,** 255.
10. Pedersen, K.S., Michelsen, M.L., and Fredheim, A.O.: "Phase equilibrium calculations for unprocessed wellstreams containing hydrate inhibitors," *Fluid Phase Equilibria* (1996) **126,** 13.
11. Pedersen, K. S., Milter, J., and Rasmussen, C.P.: "Mutual Solubility of Water and Reservoir Fluids at High Temperatures and Pressures, Experimental and Simulated Phase Equilibrium Data," *Fluid Phase Equilibria* (2001) **189,** 85.
12. Sørensen, H., Pedersen, K.S., and Christensen, P.L.: "Modeling of Gas Solubility in Brine," *Org. Geochem.* (2002) **33,** 635.
13. Michelsen, M.L.: "The Isothermal Flash, Part I and II," *Fluid Phase Equil.* (1982 a,b) **9,** 1–20, 21–40.
14. Pedersen, K.S., Blilie, A., and Meisingset, K.K.: "PVT calculations on petroleum reservoir fluids using measured and estimated compositional data for the plus fraction," *Ind. Eng. Chem. Res.* (1992) **31,** 924.

Niels Lindeloff works for Calsep in the area of modeling of PVT and phase behavior of petroleum systems. e-mail: nl@calsep.com. Previously, he spent a year as a research associate at the Technical U. of Denmark. His research interests currently include compositional grading in reservoirs and flow-assurance-related phase behavior topics such as wax deposition in pipelines, hydrates, and asphaltenes. Lindeloff holds MSc and PhD degrees in chemical engineering, both from the Technical U. of Denmark. **Michael L. Michelsen** is a professor of chemical engineering at the Technical U. of Denmark, where he has been employed since 1968. e-mail: mlm@kt.dtu.dk. He also spent a year at the U. of California, Berkeley, working on process control of chemical reactors. His research interests include mathematical modeling of chemical systems. For the last 25 years, his main research interest has been the development of algorithms for calculation of phase equilibria, in particular two-phase and multiphase flash and phase envelopes, and he is the author or coauthor of numerous articles in this field.